Mon. Not. R. Astron. Soc. **307**, 830–840 (1999)

Propagation effects on polarization of pulsar radio emission

R. T. Gangadhara,[1,2] H. Lesch[3] and V. Krishan[1]

[1]*Indian Institute of Astrophysics, Bangalore 560034, India*
[2]*National Centre for Radio Astrophysics, TIFR, Pune University Campus, Pune 411007, India*
[3]*Institut für Astronomie und Astrophysik der Universität München, Scheinerstrasse 1, 81679 München, Germany*

Accepted 1999 March 19. Received 1999 March 19; in original form 1998 May 6

ABSTRACT

We consider the role of a propagation effect such as stimulated Raman scattering on the polarization of radio pulses. When an intense electromagnetic wave with frequency close to the plasma frequency interacts with the plasma in the pulsar magnetosphere, the incident wave undergoes stimulated Raman scattering. Using typical plasma and magnetic field parameters, we compute the growth rate and estimate the polarization properties of the scattered mode. Under some conditions, we find that the polarization properties of the scattered mode can become significantly different from those of the incident wave. The frequencies at which strong Raman scattering occurs in the outer parts of the magnetosphere fall into the observable radio band. In some pulsars, for example PSR B0628−28 and B1914+13, a large and symmetric type of circular polarization has been observed. We propose that such an unusual circular polarization is produced by the propagation effects.

Key words: plasmas – polarization – radiative transfer – waves – stars: magnetic fields – pulsars: general.

1 INTRODUCTION

The investigation of coherent radio emission from pulsar magnetospheres has attracted a great deal of attention (Cordes 1979; Michel 1982; Asséo, Pelletier & Sol 1990). Powerful collective emission occurs when relativistic electron beams with density ~1 per cent of the pair plasma density scatter coherently from concentrations of plasma waves (cavitons) (Benford 1992). The role of collective plasma processes in the absorption and spectral modification of radio waves is well known (e.g. Beal 1990; Krishan & Wiita 1990; Benford 1992; Gangadhara & Krishan 1992, 1993, 1995; Gangadhara, Krishan & Shukla 1993). von Hoensbroech, Lesch and Kunzl (1998) have demonstrated that degree of linear polarization decreases with increasing frequency while the degree of circular polarization shows the opposite trend.

In this paper, we estimate the role of stimulated Raman scattering in the polarization of electromagnetic waves propagating in the pulsar magnetosphere. We assume that the physical conditions in the pulsar magnetosphere are those of the classical standard model (Ruderman & Sutherland 1975) which describes the generation of ultrarelativistic beams of electrons/positrons and the creation of the pair plasma. The beams and the pair plasma are in relativistic motion along the bundle of open magnetic field lines that delimit the active region of the magnetosphere. The stimulated Raman scattering is considered as a parametric decay of the initial transverse electromagnetic (pump) wave into another electromagnetic wave and a longitudinal plasma wave. The physics of stimulated Raman scattering in a plasma has been explained in many papers and books (e.g. Drake et al. 1974; Liu & Kaw 1976; Hasegawa 1978; Kruer 1988). There are two ways in which stimulated Raman scattering may be important in the pulsar environment. First, it may act as an effective damping mechanism for the electromagnetic waves generated by some emission mechanism at the lower altitudes in the pulsar magnetosphere. At those altitudes, the resonant conditions for stimulated Raman scattering, i.e. frequency and wavenumber matching, might not be satisfied. This results in a short time-scale of variability which is generally observed in pulsar radio emission. Secondly, stimulated Raman scattering may provide an effective saturation mechanism for the growth of the electromagnetic waves, provided that the conditions for wave excitation by some mechanism are satisfied in the region where effective stimulated Raman scattering can take place.

The first case can be simplified by treating the intensity of the pump as constant in time. Then the non-linear equations, which describe the wave coupling, become linear in the amplitudes of the decaying waves, and the exponentially growing solutions imply an effective energy transfer from the pump wave. This approximation breaks down when the amplitudes of the decay waves become comparable to that of the pump wave or when the amplitudes of the decay waves enter the non-linear stage, and start losing energy owing to some non-linear processes such as wave–particle trapping and acceleration.

The second case is more complicated, where stimulated Raman scattering acts as a non-linear saturation mechanism and the

amplitudes of all waves may be of the same order. This case can be considerably simplified when damping of the plasma wave is very strong or if it leaves the region of the resonant interaction quickly enough.

We neglect the non-linear stages of stimulated Raman scattering and the development of Langmuir turbulence, which leads to wave-particle trapping or quasi-linear diffusion. If the pump is monochromatic, the growth rate of stimulated Raman scattering can become very high, as in conventional laboratory laser–plasma interaction. However, in the case of pulsars the pump can be broadband, and, in the limit where the bandwidth $\Delta\omega$ of the pump wave is much larger than the growth rate of stimulated Raman scattering, we can use a random phase approximation for the statistical description of the interacting waves.

Tsytovich & Shvartsburg (1966) have given a general expression for the third-order non-linear currents excited in a magnetized plasma. Since the corresponding expressions are very complicated, the general case of Raman scattering becomes very difficult to consider. However, one can make some useful simplifications when considering stimulated Raman scattering in the pulsar magnetosphere. First, in a superstrong magnetic field, we can expand the currents in terms of $1/\omega_B$, where ω_B is the cyclotron frequency. Secondly, if the pair plasma has the same distributions for electrons and positrons then some of the non-linear currents cancel out, as they are proportional to the third power of the electric charge (this cancellation is exact in the unmagnetized electron–positron plasma). Thirdly, all the three interacting waves propagate along the magnetic field. This is an important but less justified approximation. It allows us to simplify the problem considerably, and to obtain a dispersion relation for stimulated Raman scattering.

The polarization of the pulsar signals appear to bear critically on the pulsar radio emission process and the emission beam geometry. One or more reversals of the sense of circular polarization have been observed in the intergrated profiles of several pulsars. However, in individual pulses, circular polarization changes sense many times across the pulse window. Further, it is important to determine whether the depolarization is a geometric effect or results from radiation–plasma interactions. There have only been very preliminary attempts to explain depolarization and microvariability using plasma mechanisms (Benford 1992).

Our purpose in this paper is to derive the properties of natural plasma modes and to explore some possible implications concerning the interpretation of the observed polarization, notably large and symmetric circular polarization in some pulsars (e.g. PSR B0628–28 and B1914+13). In Section 2, we derive the dispersion relation for stimulated Raman scattering of an electromagnetic wave, and give an analytical expression for the growth rate of the instability. In Section 3, we define the Stokes parameters and compute the polarization states of the scattered electromagnetic wave. The discussion of our findings is given in Section 4.

2 POLARIZATION CHANGES OWING TO STIMULATED RAMAN SCATTERING

We begin with a model consisting of a pulsar with a non-thermal component of radiation interacting with plasma in the emission region at a distance $r = 100R_{\rm NS} = 10^8$ cm (neutron star radius $R_{\rm NS} \approx 10$ km) from the neutron star surface, where the magnetic field is about 10^6 G. Plasma particles may all be in their lowest Landau level with no Larmor gyration; however, plasma can have one-dimensional distributions of momenta along the magnetic field (Blandford 1975; Lominadze, Machabeli & Usov 1983). This is because the synchrotron loss time for the decay of the perpendicular component of momentum is always short compared with the transit time at the stellar surface for any velocity. The simplest model for the plasma is density declining in proportion to r^{-3} with no gradients in the distribution functions across $\boldsymbol{B}$.

The non-linear interaction of radiation with plasma causes the modulation instability, leading to enhancement of non-resonant density perturbations and radiation amplification by free–electron–maser, which produces intense electromagnetic waves (Gangadhara & Krishan 1992; Gangadhara et al. 1993; Lesch, Gil & Shukla 1994). Since the frequency of these electromagnetic waves is close to the plasma frequency, they resonantly couple with the subpulse-associated plasma column in the pulsar magnetosphere and drive the stimulated Raman scattering.

Consider a large-amplitude electromagnetic wave ($\boldsymbol{k}_{\rm i}$, $\omega_{\rm i}$) with an electric field

$$\boldsymbol{E}_{\rm i} = \varepsilon_{x{\rm i}} \cos(\boldsymbol{k}_{\rm i}\cdot\boldsymbol{r} - \omega_{\rm i} t)\hat{\boldsymbol{e}}_x + \varepsilon_{y{\rm i}} \cos(\boldsymbol{k}_{\rm i}\cdot\boldsymbol{r} - \omega_{\rm i} t + \delta_{\rm i})\hat{\boldsymbol{e}}_y, \tag{1}$$

which interacts with the plasma in the pulsar magnetosphere, where ($\hat{\boldsymbol{e}}_x$, $\hat{\boldsymbol{e}}_y$) are the unit vectors, ($\epsilon_{x{\rm i}}$, $\epsilon_{y{\rm i}}$) are the x- and y- components of electric field, and $\delta_{\rm i}$ is the initial phase.

We follow Ruderman & Sutherland's (1975) approach to estimate the density and plasma frequency of the plasma moving within the bundle of field lines. For typical parameters (Lorentz factor of primary particles $\gamma_{\rm p} \sim 10^6$, and for pair plasma particles $\gamma_{\pm} \sim 10^3$, magnetic field $B_0 \sim 10^6 r_8^{-3}$ G and pulsar period $p = 1$ s), we obtain the particle number density

$$n_0 = \frac{\gamma_{\rm p}}{2\gamma_{\pm}} \frac{B_0}{ecp} = \frac{3.5\times10^7}{r_8^3} \ {\rm cm}^{-3} \tag{2}$$

and the plasma frequency

$$\omega_{\rm p} = 2\gamma_{\pm}\left(\frac{4\pi n_0 e^2}{\gamma_{\pm} m_0}\right)^{1/2} = \frac{2\times10^{10}}{r_8^{3/2}} \ {\rm rad\,s}^{-1}, \tag{3}$$

where e and m_0 are the charge and rest mass of the electron, and c is the speed of light.

The plasma in the emission region of pulsar magnetosphere may be birefringent (Melrose & Stoneham 1977; Melrose 1979; Barnard &

Arons 1986; von Hoensbroech, Lesch and Kunzl 1998). In these models, two modes of wave propagation are generally allowed in magnetoactive plasma: one mode is polarized in the $\boldsymbol{k}_i$–$\boldsymbol{B}$ plane and other mode in the direction perpendicular to it. Following these models, we resolve $\boldsymbol{E}_i$ into two modes, $\boldsymbol{E}_{xi} = \varepsilon_{xi}\cos(\boldsymbol{k}_i\cdot\boldsymbol{r} - \omega_i t)\hat{\boldsymbol{e}}_x$ and $\boldsymbol{E}_{yi} = \varepsilon_{yi}\cos(\boldsymbol{k}_i\cdot\boldsymbol{r} - \omega_i t + \delta_i)\hat{e}_y$, such that they are polarized in the directions parallel and perpendicular to the $\boldsymbol{k}_i$–$\boldsymbol{B}$ plane, respectively. It is well known from laser–plasma interactions that large-amplitude electromagnetic waves resonantly interact with the plasma when the radiation frequency becomes close to the plasma frequency. Since the two modes have different indices of refraction (McKinnon 1997), i.e. the response of plasma is not the same for the two radiation modes, it is reasonable to assume that $\boldsymbol{E}_{xi}$ couples with the density perturbation $\Delta n_1 = \delta n_1\cos(\boldsymbol{k}\cdot\boldsymbol{r} - \omega t)$, and $\boldsymbol{E}_{yi}$ couples with $\Delta n_2 = \delta n_2\cos(\boldsymbol{k}\cdot\boldsymbol{r} - \omega t + \delta)$ in the plasma medium.

Since the ponderomotive force is proportional to ∇E_{i1}^2 and ∇E_{i2}^2, the coupling between the radiation and the density perturbations is non-linear. Hence the density perturbations grow, leading to currents and mixed electromagnetic–electrostatic sideband modes at $(\boldsymbol{k}_i \pm \boldsymbol{k}, \omega_i \pm \omega)$. In turn these sideband modes couple with the incident wave field, producing a much stronger ponderomotive force, which amplifies the original density perturbation. Hence a positive feedback system sets in, which leads to an instability.

The electric field $\boldsymbol{E}_s$ of the electromagnetic wave scattered through an angle ϕ_s with respect to $\boldsymbol{k}_i$ can be written as

$$\boldsymbol{E}_s = \varepsilon_{xs}\cos(\boldsymbol{k}_s\cdot\boldsymbol{r} - \omega_s t)\hat{\boldsymbol{e}}'_x + \varepsilon_{ys}\cos(\boldsymbol{k}_s\cdot\boldsymbol{r} - \omega_s t + \delta_s)\hat{\boldsymbol{e}}'_y. \tag{4}$$

The propagation directions of the incident wave $(\boldsymbol{k}_i,\omega_i)$ and the scattered wave $(\boldsymbol{k}_s,\omega_s)$ are illustrated in Fig. 1, such that $\boldsymbol{k}_i \parallel \hat{\boldsymbol{e}}_z$, $\boldsymbol{k}_s \| \hat{\boldsymbol{e}}'_z$ and $\hat{\boldsymbol{e}}'_y \| \hat{\boldsymbol{e}}_y$. The primed coordinate system is rotated through an angle ϕ_s about the y-axis. Then the scattered wave in the unprimed coordinate system is given by

$$\boldsymbol{E}_s = \varepsilon_{xs}\cos(\phi_s)\cos(\boldsymbol{k}_s\cdot\boldsymbol{r} - \omega_s t)\hat{\boldsymbol{e}}_x + \varepsilon_{ys}\cos(\boldsymbol{k}_s\cdot\boldsymbol{r} - \omega_s t + \delta_s)\hat{\boldsymbol{e}}_y - \varepsilon_{zs}\sin(\phi_s)\cos(\boldsymbol{k}_s\cdot\boldsymbol{r} - \omega_s t)\hat{\boldsymbol{e}}_z, \tag{5}$$

where $\varepsilon_{zs}=\varepsilon_{xs}$.

The quiver velocity $\boldsymbol{u}_\pm$ of positrons and electrons owing to the radiation fields $\boldsymbol{E}_i$ and $\boldsymbol{E}_s$ is given by

$$\frac{\partial \boldsymbol{u}_\pm}{\partial t} = \pm\frac{e}{m_0}(\boldsymbol{E}_i + \boldsymbol{E}_s), \tag{6}$$

where e and m_0 are the charge and rest mass of the plasma particle.

The wave equation for the scattered electromagnetic wave is given by

$$\left(\nabla^2 - \frac{1}{c^2}\frac{\partial^2}{\partial t^2}\right)\boldsymbol{E}_s = \frac{4\pi}{c^2}\frac{\partial \boldsymbol{J}}{\partial t}, \tag{7}$$

where c is the velocity of light and $\boldsymbol{J}$ is the current density.

The components of equation (7) are

$$D_s\varepsilon_{xs}\cos(\phi_s)\cos(\boldsymbol{k}_s\cdot\boldsymbol{r} - \omega_s t) = -\frac{2\pi e^2}{m_0}\frac{\omega_s}{\omega_i}\varepsilon_{xi}\delta n_1\cos(\boldsymbol{k}_s\cdot\boldsymbol{r} - \omega_s t), \tag{8}$$

$$D_s\varepsilon_{ys}\cos(\boldsymbol{k}_s\cdot\boldsymbol{r} - \omega_s t + \delta_s) = -\frac{2\pi e^2}{m_0}\frac{\omega_s}{\omega_i}\varepsilon_{yi}\delta n_2\cos(\boldsymbol{k}_s\cdot\boldsymbol{r} - \omega_s t + \delta_i - \delta) \tag{9}$$

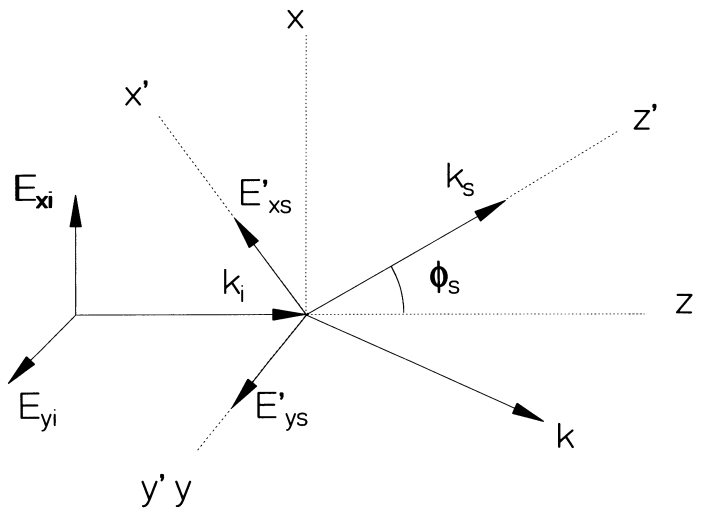

Figure 1. Stimulated Raman scattering of a transverse electromagnetic wave ($\boldsymbol{E}_{xi}$, $\boldsymbol{E}_{yi}$) through an angle ϕ_s. The scattered wave electric field is ($\boldsymbol{E}_{xs}$, $\boldsymbol{E}_{ys}$). The wavenumbers $\boldsymbol{k}_i$, $\boldsymbol{k}_s$ and $\boldsymbol{k}$ are due to the incident, scattered and Langmuir waves, respectively.

and

$$D_s \varepsilon_{zs} \sin(\phi_s) \cos(\boldsymbol{k}_s \cdot \boldsymbol{r} - \omega_s t) = 0, \tag{10}$$

where $D_s = k_s^2 c^2 - \omega_s^2 + \omega_p^2$ and

$$\omega_s = \omega_i - \omega, \quad \boldsymbol{k}_s = \boldsymbol{k}_i - \boldsymbol{k}. \tag{11}$$

In quantum language these two relations may be interpreted as the conservation of energy and the momentum along the magnetic field, respectively. When these conditions are satisfied, stimulated Raman scattering is excited resonantly and the expression $D_s \approx 0$ becomes the dispersion relation of the scattered electromagnetic mode.

If we cancel the instantaneous space- and time-dependent cosine functions on both sides of equation (8), we get

$$D_s \varepsilon_{xs} \cos(\phi_s) = -\frac{2\pi e^2}{m_0} \frac{\omega_s}{\omega_i} \varepsilon_{xi} \delta n_1. \tag{12}$$

Similar to the phase matching conditions (equation 11), equation (9) gives the condition between the initial phases:

$$\delta_s = \delta_i - \delta, \tag{13}$$

and hence we obtain

$$D_s \varepsilon_{ys} = -\frac{2\pi e^2}{m_0} \frac{\omega_s}{\omega_i} \varepsilon_{yi} \delta n_2. \tag{14}$$

Dividing equation (14) by equation (12), we have

$$\alpha_s = \alpha_i \eta \cos(\phi_s), \tag{15}$$

where $\alpha_i = \varepsilon_{yi}/\varepsilon_{xi}$, $\alpha_s = \varepsilon_{ys}/\varepsilon_{xs}$ and $\eta = \delta n_2/\delta n_1$. The value of η is determined by $\boldsymbol{E}_i$ in such a way that Δn_1 couples with $\boldsymbol{E}_{xi}$ and Δn_2 couples with $\boldsymbol{E}_{yi}$.

We consider the Vlasov equation to find the low-frequency plasma response:

$$\frac{\partial f}{\partial t} + \boldsymbol{v} \cdot \nabla f + \frac{1}{m_0} (e\nabla\phi - \nabla\psi) \cdot \frac{\partial f}{\partial \boldsymbol{v}} = 0, \tag{16}$$

where $\phi(\boldsymbol{r},t)$ is the scalar potential associated with the electrostatic waves, $f(\boldsymbol{r},\boldsymbol{v},t)$ is the particle distribution function and $\psi(\boldsymbol{r},t)$ is the ponderomotive potential.

Using $f(\boldsymbol{r},\boldsymbol{v},t) = f_0(\boldsymbol{v}) + \Delta f_1(\boldsymbol{r},\boldsymbol{v},t) + \Delta f_2(\boldsymbol{r},\boldsymbol{v},t)$, we can linearize equation (16), and obtain

$$\frac{\partial(\Delta f_1)}{\partial t} + \frac{\partial(\Delta f_2)}{\partial t} + \boldsymbol{v} \cdot \nabla(\Delta f_1) + \boldsymbol{v} \cdot \nabla(\Delta f_2) + \frac{1}{m_0} (e\nabla\phi - \nabla\psi) \cdot \frac{\partial f_0}{\partial \boldsymbol{v}} = 0, \tag{17}$$

where $\Delta f_1 = \delta f_1 \cos(\boldsymbol{k}\cdot\boldsymbol{r} - \omega t)$ and $\Delta f_2 = \delta f_2 \cos(\boldsymbol{k}\cdot\boldsymbol{r} - \omega t + \delta)$. The ponderomotive force of the radiation field depends quadratically on the amplitude of the electric field. Physically, it is a radiation pressure which amplifies the density perturbations by exciting the slow longitudinal fields and motions. The ponderomotive potential is given by

$$\psi = \frac{e^2}{2m_0} \left\langle \left(\mathrm{Re} \left| \frac{\boldsymbol{E}_i}{i\omega_i} + \frac{\boldsymbol{E}_s}{i\omega_s} \right| \right)^2 \right\rangle_\omega = \frac{e^2}{2m_0\omega_i^2} [\cos(\phi_s) \cos(\boldsymbol{k}\cdot\boldsymbol{r} - \omega t) + \alpha_i \alpha_s \cos(\boldsymbol{k}\cdot\boldsymbol{r} - \omega t + \delta_i - \delta_s)] \varepsilon_i \varepsilon_s, \tag{18}$$

where the brackets $\langle\ \rangle_\omega$ represent the average over the fast time-scale ($\omega_i \gg \omega$).

In the presence of a strong magnetic field, the pair plasma becomes polarized and one-dimensional. If there is some relativistic drift between the electrons and the positrons then the ponderomotive force becomes effective, which will induce the non-linear density perturbations (Asséo 1993):

$$\delta n_\pm \approx -\frac{1}{32\pi} \frac{|\varepsilon_\parallel|^2}{k_B T_p} \frac{\omega_p^2}{\omega_i^2} \frac{1}{\gamma_\pm}, \tag{19}$$

where $\varepsilon_\parallel$ is the envelope of the parallel electric field of the Langmuir wave which is slowly varying with space and time, and T_p is the plasma temperature. Using these density perturbations and Poisson equation, we can self-consistently derive the potential ϕ:

$$\phi = -\frac{4\pi e}{k^2} (\Delta n_1 + \Delta n_2). \tag{20}$$

Now, substituting the expressions for Δf_1, Δf_2, Δn_1, Δn_2, ϕ and ψ into equation (17) and using the condition (13), we obtain

$$\delta f_2 + \delta f_1 \mu + \left\{ \frac{4\pi e^2}{m_0 k^2} (\delta n_2 + \delta n_1 \mu) + \frac{e^2}{2m_0^2\omega_i^2} [\cos(\phi_s)\mu + \alpha_i \alpha_s] \varepsilon_i \varepsilon_s \right\} \frac{\boldsymbol{k} \cdot \frac{\partial f_0}{\partial \boldsymbol{v}}}{(\omega - \boldsymbol{k}\cdot\boldsymbol{v})} = 0, \tag{21}$$

where $\mu = \sin(\boldsymbol{k}\cdot\boldsymbol{r} - \omega t)/\sin(\boldsymbol{k}\cdot\boldsymbol{r} - \omega t + \delta)$. For $\delta = 0$ and π, $\mu = \pm 1$, while at the other values of δ we have to find the average $\langle\mu\rangle = \mu_a$ over the time-scale $T = 2\pi/\omega$. Therefore we have

$$\delta f_2 + \delta f_1 \mu_a = -\frac{4\pi e^2}{m_0 k^2}\left(\delta n_2 + \delta n_1 \mu_a + \frac{\varepsilon_i k^2}{8\pi m_0 \omega_i^2} A\right)\frac{\boldsymbol{k}\cdot\dfrac{\partial f_0}{\partial \boldsymbol{v}}}{(\omega - \boldsymbol{k}\cdot\boldsymbol{v})}, \tag{22}$$

where $A = (\mu_a \cos\phi_s + \alpha_i \alpha_s)\varepsilon_s$. The sum of density perturbations $(\delta n_2 + \delta n_1 \mu_a)$ can be estimated as

$$\delta n_2 + \delta n_1 \mu_a = \int_{-\infty}^{\infty} n_0 (\delta f_2 + \delta f_1 \mu_a) \mathrm{d}\boldsymbol{v} = -\left[\delta n_2 + \delta n_1 \mu_a + \frac{\varepsilon_i k^2}{8\pi m_0 \omega_i^2} A\right]\chi, \tag{23}$$

where

$$\chi = \frac{\omega_p^2}{k^2}\int_{-\infty}^{\infty} \frac{\boldsymbol{k}\cdot\dfrac{\partial f_0}{\partial \boldsymbol{v}}}{(\omega - \boldsymbol{k}\cdot\boldsymbol{v})} \mathrm{d}\boldsymbol{v} \tag{24}$$

is the susceptibility function (Fried & Conte 1961; Liu & Kaw 1976). Using $\eta = \delta n_2/\delta n_1$, we can write

$$\left(1 + \frac{1}{\chi}\right)(\eta + \mu_a)\delta n_1 = -\frac{\varepsilon_i k^2}{8\pi m_0 \omega_i^2} A. \tag{25}$$

Multiplying equation (12) by $\varepsilon_i \mu_a$ and equation (14) by $\alpha_i \varepsilon_i$, and adding, we get

$$(\alpha_s \alpha_i + \mu_a \cos\phi_s)\varepsilon_s = -\frac{2\pi e^2}{m_0}\frac{\omega_s}{\omega_i}\varepsilon_i(\mu_a + \alpha_i^2 \eta)\frac{\delta n_1}{D_s}, \tag{26}$$

where $\varepsilon_i = \varepsilon_{xi}$ and $\varepsilon_s = \varepsilon_{xs}$.

Now, using equations (25) and (26), we obtain the dispersion relation for stimulated Raman scattering:

$$\left(1 + \frac{1}{\chi}\right)(\eta + \mu_a) = \frac{v_0^2 k^2}{4}\frac{(\mu_a + \alpha_i^2 \eta)}{(1 + \alpha_i^2)}\frac{\omega_s}{\omega_i}\frac{1}{D_s}, \tag{27}$$

where $v_0 = e\varepsilon_i\sqrt{1 + \alpha_i^2}/m_0\omega_i$ is the quiver velocity of plasma particles owing to the electric field of the incident electromagnetic wave.

If $L = L_{30} \times 10^{30}\mathrm{ergs}^{-1}$ is the luminosity of pump radiation with frequency $\omega_i = 2\pi\nu_i = \nu_{10} \times 10^{10}\,\mathrm{rad\,s}^{-1}$ at a distance $r = r_8 \times 10^8\,\mathrm{cm}$ from the source then

$$v_0 = \frac{e}{m_0 \omega_i}\left(\frac{2L}{r^2 c}\right)^{1/2} = 4.3 \times 10^9 \frac{L_{30}^{1/2}}{\nu_{10} r_8}\,\mathrm{cm\,s}^{-1}. \tag{28}$$

When the phase matching conditions are met, the instability becomes more efficient, and $D_s = 2\omega_i\omega - \omega^2 - 2c^2\boldsymbol{k}_i\cdot\boldsymbol{k} + c^2k^2 \approx 0$ represents the dispersion relation of the Stokes mode.

The thermal speed v_t of the plasma can be expressed in terms of its energy spread in the laboratory frame. Let $v_\pm = c(1 - 1/\gamma_\pm^2)^{1/2}$ be the velocity of the electron–positron plasma; then the velocity spread $\delta v_\pm$ is given by (Hasegawa 1978; Gangadhara & Krishan 1992)

$$\delta v_\pm \approx c\frac{\delta\gamma_\pm}{\gamma^3} \quad \text{for } \gamma \gg 1. \tag{29}$$

Now, using the Lorentz transformation of velocity, we can show that

$$\delta v_\pm = \delta v_z = \frac{\delta v_z'}{\gamma_\pm^2(1 + v_\pm v_z'/c^2)} \approx \frac{\delta v_z'}{\gamma^2} = \frac{v_t}{\gamma^2} \tag{30}$$

because $v_z' = 0$. Hence the thermal speed, in the plasma frame, is given by

$$v_t = c\frac{\delta\gamma_\pm}{\gamma_\pm}. \tag{31}$$

For $\gamma_\pm = 10^3$, we get $v_t = 3 \times 10^7 \delta\gamma_\pm\,\mathrm{cm\,s}^{-1}$.

If we separate equation (27) into real and imaginary parts, we get two coupled simultaneous equations. By solving them numerically, we find the growth rate Γ of stimulated Raman scattering. Fig. 2 shows the growth rate as a function of r_8 and ω_i/ω_p. Since the plasma density decreases with r as $1/r^3$, the growth rate decreases as r_8 increases. Also, if the radiation frequency becomes higher than the plasma frequency, then radiation and plasma do not couple resonantly, which leads to the decrease of the growth rate at higher values of ω_i/ω_p.

To study the variation of Γ in the α_i–$\delta\gamma_\pm$ plane, we have made a contour plot (Fig. 3); the labels on the contours indicate the values of log (Γ). The Debye length increases with the increase of $\delta\gamma_\pm$, therefore the plasma wave experiences a large Landau damping, which leads to the drop in growth rate. The parameter α_i is the ratio of amplitudes of electromagnetic waves that are polarized in the directions parallel and perpendicular to the $\boldsymbol{k}_i$–$\boldsymbol{B}$ plane. When α_i is small, the wave polarized in the direction parallel to the $\boldsymbol{k}_i$–$\boldsymbol{B}$ plane becomes strong and

will have a component along $\boldsymbol{B}$. Therefore the coupling between radiation and plasma will be strong, which leads to the higher growth rate at the smaller values of α_i.

For $\omega \ll c^2\boldsymbol{k}_i\cdot\boldsymbol{k}/\omega_i$, Stokes mode becomes resonant, and the anti-Stokes mode becomes non-resonant. Then equation (27) can be written as

$$(\omega - \omega_l + i\Gamma_l)(\omega - \omega_l + i\Gamma_s)(\eta + \mu_a) = -10^{18}\frac{L_{30}}{r_8^{7/2}\nu_{10}}\frac{(\mu_a + \alpha_i^2\eta)}{(1+\alpha_i^2)}\ \mathrm{rad}^2\,\mathrm{s}^{-2}, \tag{32}$$

where $\omega_l^2 = \omega_p^2 + (3/2)k^2v_t^2$,

$$\Gamma_l = \frac{\sqrt{\pi}}{2}\frac{\omega_p}{(k\lambda_D)^3}\exp\left[-\frac{1}{2(k\lambda_D)^2} - \frac{3}{2}\right] + \nu_c \tag{33}$$

is the damping rate of the plasma wave, and the Debye length $\lambda_D = v_t/\sqrt{2}\omega_p$. For $k\lambda_D \sim 1$, we find $\Gamma_l \approx 2.5\times10^9/r_8^{3/2}\mathrm{s}^{-1}$. The pair plasma collision frequency $\nu_c \approx 2.5\times10^{-3}\ln\Lambda/r_8^3\delta\gamma_\pm^3\ \mathrm{s}^{-1}$ and the Coulomb logarithm $\ln\Lambda \approx 10$. The collisional damping rate of the scattered electromagnetic wave is given by $\Gamma_s = \omega_p^2\nu_c/2\omega_s^2 \approx 0.06/\nu_{10}^2r_8^6\delta\gamma_\pm^3\,\mathrm{s}^{-1}$.

For $k\lambda_D > 1$, plasma waves are highly damped and hence the plasma loses its collective behaviour. Therefore stimulated Raman scattering changes into induced Compton scattering of electromagnetic waves by the plasma particles. In the conventional treatment of induced Compton scattering in pulsars (e.g. Blandford & Scharlemann 1976; Sincell & Krolik 1992) the collective effects of the plasma are ignored. The collective treatment of the wave scattering by plasma particles is justified if the condition $k\lambda_D \ll 1$ or $v_{ph} \gg v_t$ is met, where $v_{ph} = w_p/k$ is the phase velocity of the plasma wave. This condition implies that the wavenumber of oscillation of the electrons in the beat wave of the incident and scattered waves is much less than the inverse of the Debye length. It is not satisfied when the beat wave is strongly Landau damped ($k\lambda_D > 1$) or the beat wave will not feel the presence of a medium ($k\lambda_D \gg 1$), so that the scattering process will be described as induced Compton scattering.

When $k\lambda_D \ll 1$, by setting $\omega = \omega_l + i\Gamma$, we can solve equation (32) for the growth rate:

$$\Gamma = -\frac{1}{2}(\Gamma_l + \Gamma_s) \pm \frac{1}{2}\sqrt{(\Gamma_l - \Gamma_s)^2 + 4.3\times10^{18}\frac{L_{30}}{r_8^{7/2}\nu_{10}}\frac{(\mu_a + \alpha_i^2\eta)}{(1+\alpha_i^2)(\eta+\mu_a)}}\,. \tag{34}$$

Stimulated Raman scattering is a threshold process: if the intensity of the pump exceeds the threshold, only then will it start converting its energy into decay waves. The threshold condition for the excitation of stimulated Raman scattering is given by

$$\left(\frac{L_{30}}{r_8^2}\right)_{thr} = 9.3\times10^{-19}\nu_{10}r_8^{3/2}\Gamma_l\Gamma_s\frac{(1+\alpha_i^2)(\eta+\mu_a)}{(\mu_a + \alpha_i^2\eta)}. \tag{35}$$

The typical threshold intensities for stimulated Raman scattering are of the order of the observed intensities, implying that pulsar magnetosphere may be optically thick to Raman scattering of electromagnetic waves.

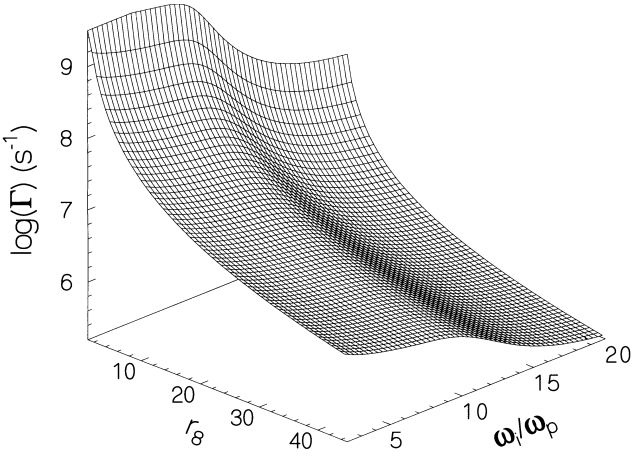

Figure 2. The growth rate Γ of stimulated Raman scattering is plotted with respect to r_8 and ω_i/ω_p.

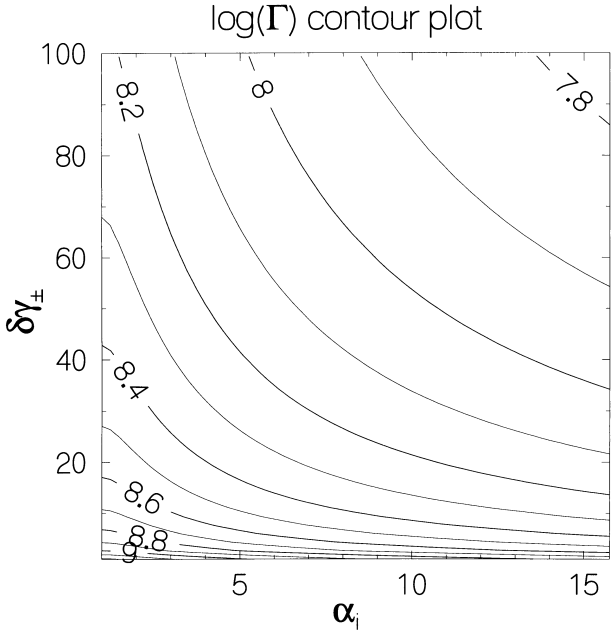

Figure 3. A contour plot of Γ in the $\delta_\pm - \alpha_i$ plane. The labels on the contours indicate the log (Γ) values.

The growth rate just above the threshold is given by

$$\Gamma = 4.3 \times 10^8 \frac{L_{30}}{r_8^2 \nu_{10}} \frac{(\mu_a + \alpha_i^2 \eta)}{(1 + \alpha_i^2)(\eta + \mu_a)} \ \mathrm{s}^{-1}, \tag{36}$$

which is proportional to L_{30}. The maximum growth rate attainable for $\omega_p > \Gamma > \Gamma_l$, on the other hand, is

$$\Gamma = 10^9 \sqrt{\frac{L_{30}}{\nu_{10}^3 r_8^{13/2}} \frac{(\mu_a + \alpha_i^2 \eta)}{(1 + \alpha_i^2)(\eta + \mu_a)}} \ \mathrm{s}^{-1}. \tag{37}$$

3 STOKES PARAMETERS

When the phase matching conditions are satisfied, the growth rate Γ becomes large, and the scattered mode is amplified and becomes a normal mode of the plasma. Under some conditions, the scattered mode leaves the plasma with a polarization which may be different from the polarization of the incident wave. The polarization states of the incident and scattered waves can be described more accurately using the Stokes parameters (Rybicki & Lightman 1979):

$$I_j = \varepsilon_{xj} \varepsilon_{xj}^* + \varepsilon_{yj} \varepsilon_{yj}^*, \tag{38}$$

$$Q_j = \varepsilon_{xj} \varepsilon_{xj}^* - \varepsilon_{yj} \varepsilon_{yj}^*, \tag{39}$$

$$U_j = 2 \varepsilon_{xj} \varepsilon_{yj}^* \cos(\delta_j) \tag{40}$$

and

$$V_j = 2 \varepsilon_{xj} \varepsilon_{yj}^* \sin(\delta_j), \tag{41}$$

where $j = \mathrm{i}$ for the incident wave, and s for the scattered wave. The linear polarization is given by

$$L = \sqrt{U_j^2 + Q_j^2}, \tag{42}$$

and the polarization position angle is given by

$$\chi_j = \frac{1}{2} \arctan(U_j / Q_j). \tag{43}$$

The transfer of energy between the modes will be efficient only when the energy of the pump wave is strong enough to overcome the damping losses or escape of the generated waves. Using the Manley–Rowe relation (Weiland & Wilhelmsson 1977)

$$\frac{I_i}{\omega_i} = \frac{I_s}{\omega_s}, \tag{44}$$

we find the relation between the incident flux I_i and the scattered flux I_s:

$$I_s = \left(1 - \frac{\omega}{\omega_i}\right) I_i. \tag{45}$$

In the following two subsections, we consider the cases in which the polarization state of the incident wave is linear and circular, and compute the polarization states of the scattered mode.

3.1 Linearly polarized incident wave

Consider a linearly polarized electromagnetic wave ($\delta_i = 0$, $\alpha_i = 10$ and $\chi_i = 90°$), which excites stimulated Raman scattering in the magnetospheric plasma. Using the plasma and magnetic field parameters discussed in the previous section, we compute the growth rate of stimulated Raman scattering. For $k\lambda_D \ll 1$, the instability becomes quite strong and the Landau damping of the Langmuir wave is minimal. Hence the stimulated Raman scattering is resonantly excited. Fig. 4 shows the behaviour of linear (solid line) and circular (broken line) polarization of the scattered mode with respect to η. It shows that, at some values of η which are close to 0.1, the linear polarization of the incident wave can be converted almost completely into circular polarization of the scattered wave. Charge density variations within the pulse window could cause the conversion efficiency of linear to circular polarization to vary.

The variation of the polarization angle of the scattered wave with respect to η, at different values of δ, is shown in Fig. 5. For $\delta = 90°$ and $\eta \leq 0.1$, the scattered mode becomes orthogonally polarized with respect to the incident wave. Furthermore, if there is any variation in the plasma density or radiation intensity, the value of η fluctuates and the scattered modes produced with $\eta \leq 0.1$ become orthogonally polarized with respect to those produced with $\eta > 0.1$.

3.2 Circularly polarized incident wave

Suppose that the incident wave is circularly polarized ($\delta_i = \pi/2$ and $\alpha_i = 1$); then the scattered mode will be linearly polarized for $\eta \leq 0.2$, while, at the other values, both linear and circular polarizations with different proportions will exist, as indicated by Fig. 6. For $\delta_i < 0$ and $\delta_s = \delta_i - \delta < 0$ the sense of circular polarization of the scattered mode becomes opposite to that of the incident wave. Hence, depending upon the plasma and radiation conditions, stimulated Raman scattering can change the polarization of the pulsar radio signals.

4 DISCUSSION

The variable nature of circular polarization is evident from the polarization distributions of Manchester, Taylor & Huguenin (1975), Backer & Rankin (1980)and Stinebring et al. (1984a,b). Very high degrees of circular polarization are occasionally observed in individual pulses, even up to 100 per cent (Cognard et al. 1996), while the integrated or average pulse profiles generally indicate a much smaller degree of circular polarization (e.g. Lyne, Smith & Graham 1971), which show that the sign of circular polarization is variable at any given pulse phase. Radhakrishnan & Rankin (1990) have identified two extreme types of circular polarization in the observations: (i) an antisymmetric type wherein the circular polarization changes sense in mid-pulse; and (ii) a symmetric type wherein it is predominantly of one sense. The correlation of sense of the antisymmetric type of circular polarization with the polarization angle swing indicates the geometric property of the emission process, and is highly suggestive of curvature radiation.

The diverse nature of circular polarization may be the consequence of the pulsar emission mechanism and the subsequent propagation effects in the pulsar magnetosphere (e.g. Melrose 1995; von Hoensbroech, Lesch & Kunzl 1998). It seems rather difficult to explain the various circular polarization behaviours using the widely accepted magnetic pole models (e.g. Radhakrishnan & Cooke 1969; Komesaroff 1970; Sturrock 1971; Ruderman & Sutherland 1975).

The symmetric type of circular polarization observed in some pulsars (e.g. PSR B1914+13 and B0628–28), as shown in Figs 7 and 8, may be due to the propagation effects. However, it seems difficult for propagation effects to explain how the sign of the circular polarization can change precisely at the centre of the pulse in the case of the antisymmetric type, as seen in many pulsars, e.g. PSR B1859+03 and B1933+16 (Rankin, Stinebring & Weisberg 1989).

If we are to understand the radio emission mechanism, we must understand the physical state of the radio-loud plasma in the polar cap. It is this plasma that is the site of instabilities which are thought to produce coherent radio emission. The role of different propagation effects in the pulsar polarization has been discussed by Cheng & Ruderman (1979), Beskin, Gurevich & Istomin (1988) and Istomin (1992). The mechanisms proposed by these authors predict a frequency dependence for circular polarization, with weaker polarization at higher frequencies. This is seen in some pulsars (e.g. PSR B0835–41, B1749–28 and B1240–64), but it is not generally the case (Han et al. 1998). Istomin suggested that the linearly polarized incident wave becomes circularly polarized as a result of generalized Faraday rotation; however, it is observationally known that no generalized Faraday rotation is evident in pulsar magnetospheres (Cordes 1983; Lyne & Smith 1990).

We have presented a model to explain the polarization changes owing to the propagation of radio waves through the magnetospheric

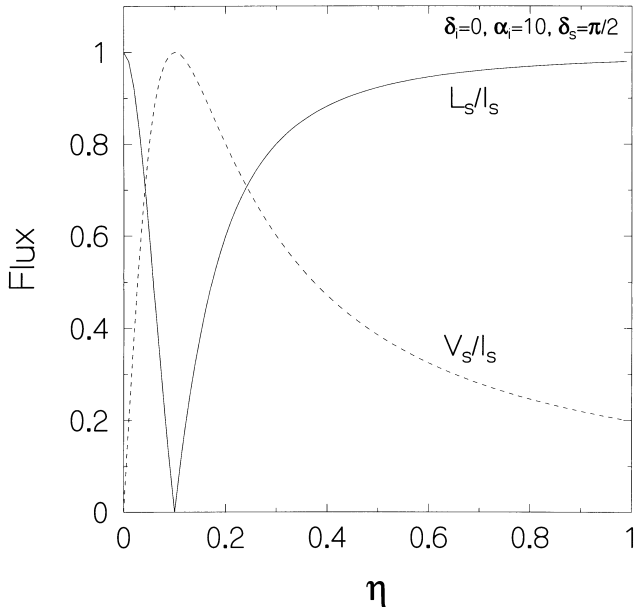

Figure 4. The solid line and broken curves indicate the variation of linear (L_s) and circular (V_s) polarization of the scattered mode with respect to η. The normalizing parameter I_s is the intensity of the scattered mode.

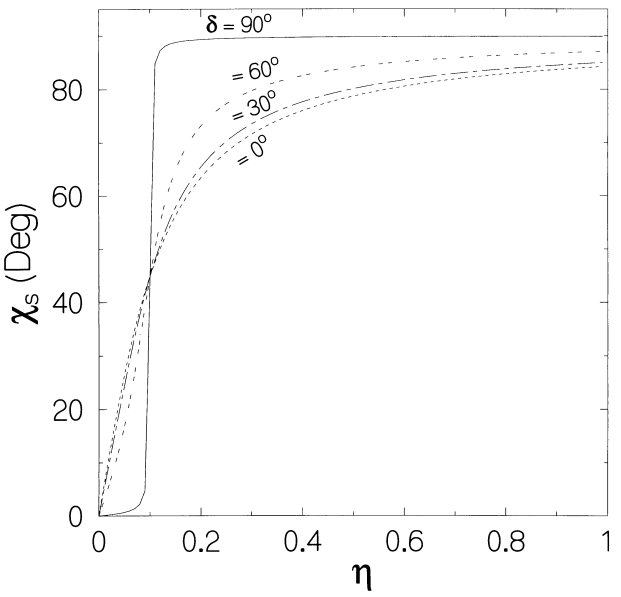

Figure 5. The polarization angle χ_s of the scattered mode is plotted as a function of η, at different values of δ (0°, 30°, 60° and 90°).

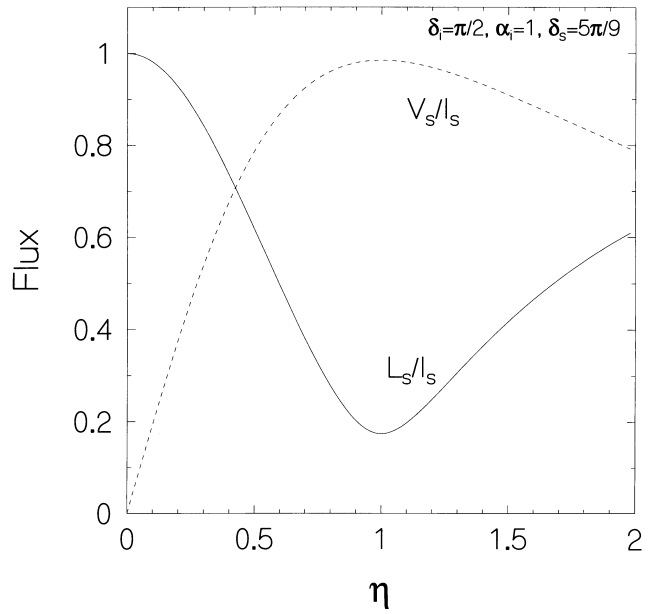

Figure 6. The variation of linear (L_s) and circular (V_s) polarization of the scattered mode, with respect to η, indicated by the solid line and broken curves, respectively. The normalizing parameter I_s is the intensity of the scattered mode.

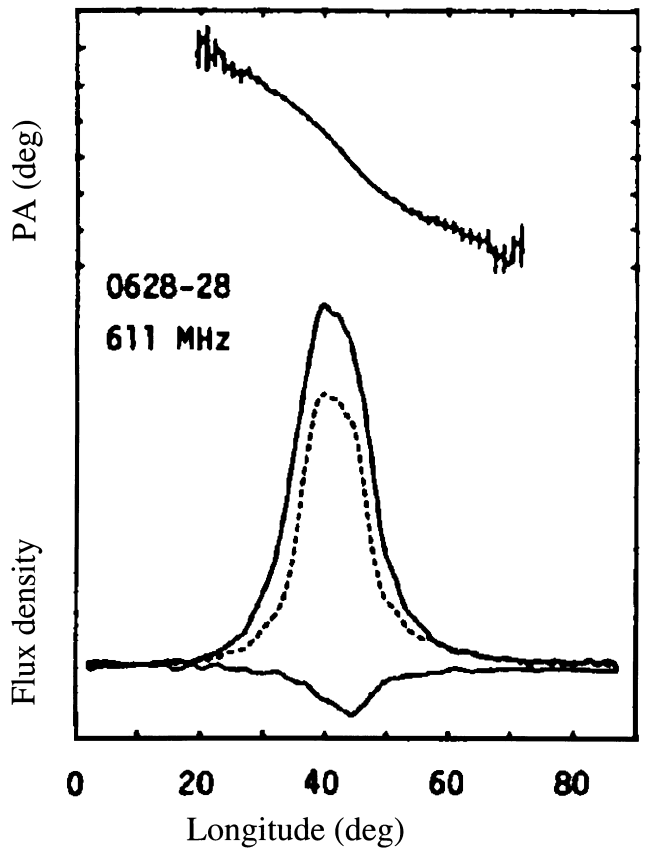

Figure 7. PSR B0628–28, an example of a pulsar with 'symmetric' circular polarization and high linear polarization (from Lyne & Manchester 1988).

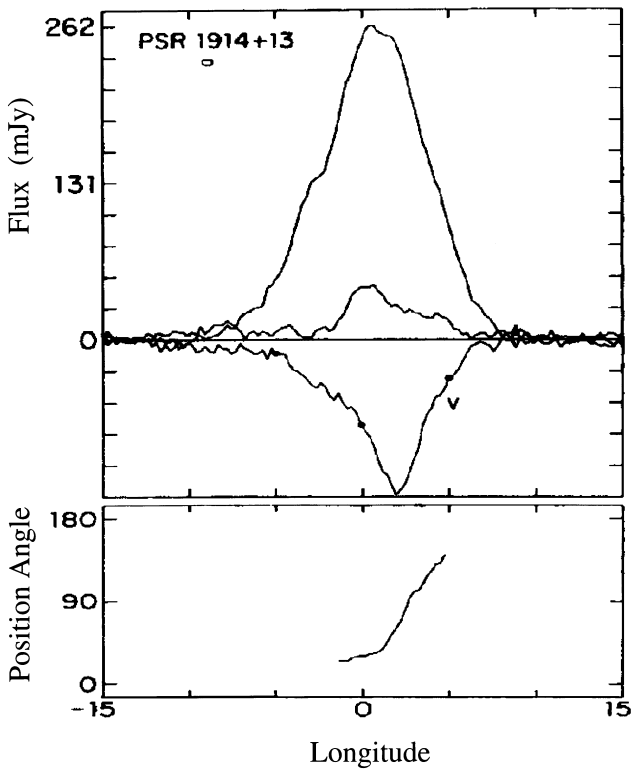

Figure 8. The polarization of PSR B1914+13, a pulsar with strong circular polarization over the whole observed profile (from Rankin et al. 1989).

plasma. The features, like a large change in polarization angle, a sense reversal of circular polarization and extremely rapid temporal changes in intensity, would help us to explain many observations, for which the existing mechanisms have proved to be inadequate. Because of the very strong dependence of polarization angle on plasma parameters via the growth rate, in an inhomogeneous plasma medium the depolarization is a natural outcome. We believe that plasma processes such as the stimulated Raman scattering may be a potential mechanism for the polarization variability in pulsars. The circular polarization of a number of pulsars varies with frequency. The two clear

examples are PSR B1240−64 and B2048−78, from which the opposite senses or transitions of circular polarization have been observed at lower and higher frequencies in the radio band (Han et al. 1998).

5 CONCLUSION

We have considered the stimulated Raman scattering of the transverse electromagnetic waves in the electron–positron plasma of a pulsar magnetosphere. Since the frequency of the incident wave is much higher than the plasma frequency in stimulated Raman scattering, the change in scattered wave frequency is very small compared with the incident wave frequency. The value of the radiation–plasma coupling parameter η is determined by the polarization of the incident wave, and its value can be determined only by non-linear analysis. In the process of three-wave interaction, the phase matching condition (equation 13) between the initial phases (δ_i, δ_s, δ) and the value of η determine the polarization state of the scattered wave.

Many short-time-scale polarization variabilities in individual pulses, such as variations in the amount of linear and circular polarization, a sense reversal of circular polarization, and polarization angle swings, can be accounted for by considering stimulated Raman scattering. The time-scales over which the changes take place in individual pulses are of the order of the e-folding time, which is the inverse of the growth rate of stimulated Raman scattering.

It seems rather unlikely that the diverse behaviour of circular polarization can be accounted for by a single mechanism. Both intrinsic emission and propagation effects seem possible. The strong symmetric type of circular polarization observed in some pulsars is most probably generated by propagation effects, such as stimulated Raman scattering. Further simultaneous observations over a wide frequency range would be valuable in sorting out the importance of propagation effects.

ACKNOWLEDGMENTS

We are grateful to Y. Gupta and A. von Hoensbroech for discussions and comments. Fig. 8 has been reproduced, with permission, from Astrophysical Journal, published by The University of Chicago Press. (© 1989 by the American Astronomical Society. All rights reserved.) We thank Dr. J. M. Rankin for allowing us to use Fig. 8.

REFERENCES

Asséo E., 1993, MNRAS, 264, 940
Asséo E., Pelletier G., Sol H., 1990, MNRAS, 247, 529
Backer D. C., Rankin J. M., 1980, ApJS, 42, 143
Barnard J. J., Arons J., 1986, ApJ, 302, 138
Beal J. H., 1990, in Brinkmann W., Fabian A. C., Giovannelli F., eds, Physical Processes in Hot Cosmic Plasmas. Kluwer, Dordrecht, p. 341
Benford G., 1992, ApJ, 391, L59
Beskin V. S., Gurevich A. V., Istomin Ya. N., 1988, Ap. C&SS, 146, 205
Blandford R. D., Scharlemann E. T., 1976, MNRAS, 174, 59
Blandford R. D., 1975, MNRAS, 170, 551
Cheng A. F., Ruderman M. A., 1979, ApJ, 229, 348
Cognard I., Shrauner J. A., Taylor J. H., Thorsett S. E., 1996, ApJ, 457, L81
Cordes J. M., 1979, Space Sci. Rev., 24, 567
Cordes J. M., 1983, in Burns M. L., Harding A. K., Ramaty R., eds, AIP Conf. Proc. 101, Positron–Electron pairs in Astrophysics. Am. Inst. Phys., New York, p. 98
Drake J. F., Kaw P. K., Lee Y. C., Schmidt G., Liu C. S., Rosenbluth M. N., 1974, Phys. Fluids, 17, 778
Fried D., Conte S. D., 1961, The Plasma Dispersion Function. Academic Press, New York, p. 1
Gangadhara R. T., Krishan V., 1992, MNRAS, 256, 111
Gangadhara R. T., Krishan V., 1993, ApJ, 415, 505
Gangadhara R. T., Krishan V., 1995, ApJ, 440, 116
Gangadhara R. T., Krishan V., Shukla P. K., 1993, MNRAS, 262, 151
Han J. L., Manchester R. N., Xu R. X., Qiao G. J., 1998, MNRAS, 300, 373
Hasegawa A., 1978, Bell System Tech. J., 57, 3069
Istomin Ya. N., 1992, in Hankins T. H., Rankin J. M., Gil J. A., eds, Proc. IAU Colloq. 128, The magnetosphere structure and emission mechanism of radio pulsars. Pedagogical Univ. Press, Zielona Góra, p. 375
Komesaroff M. M., 1970, Nat, 225, 612
Krishan V., Wiita P. J., 1990, MNRAS, 246, 597
Kruer W. L., 1988, The Physics of Laser–plasma interactions. Addison-Wesley, New York, p. 70
Lesch H., Gil J. A., Shukla P. K., 1994, Space Sci. Rev., 68, 349
Liu C.S., Kaw P.K. 1976, in Simon, A., Thompson W. B., eds, Advances in Plasma Physics. Interscience, New York, Vol. 6, p. 83
Lominadze Dzh. G., Machabeli G. Z., Usov V. V. 1983, ApS&S, 90, 19
Lyne A. G., Manchester R. N., 1988, MNRAS, 234, 477
Lyne A. G., Smith F. G., 1990, Pulsar Astronomy, Cambridge Univ. Press, Cambridge, 234
Lyne A. G., Smith F. G., Graham D. A., 1971, MNRAS, 153, 337
McKinnon 1997, ApJ, 475, 763
Manchester R. N., Taylor J. H., Huguenin G. R., 1975, ApJ, 196, 83

Melrose D. B., Aust 1979, J. Phys. 32, 61
Melrose D. B., Stoneham M. M., 1977, Proc. Astron. Soc. Aust., 3, 120
Melrose D. B., 1995, JA&A, 16, 137
Michel F. C., 1982, Rev. Mod. Phys., 54, 1
Radhakrishnan V., Cooke D. J., 1969, Astrophys. Lett. 3, 225
Radhakrishnan V., Rankin J. M., 1990, ApJ, 352, 258
Rankin J. M., Stinebring D. R., Weisberg J. M., 1989, ApJ, 346, 869
Ruderman M., Sutherland P., 1975, ApJ, 196, 51
Rybicki G. B., Lightman A. P., 1979, Radiative Processes in Astrophysics. Wiley-Interscience, p. 62
Sincell M. W., Krolik J. H., 1992, ApJ, 395, 553
Stinebring D. R., Cordes J. M., Rankin J. M., Weisberg J. M. Boriakoff V., 1984a, ApJS, 55, 247
Stinebring D. R. Cordes J. M., Weisberg J. M., Rankin J. M., Boriakoff V., 1984b, ApJS, 55, 279
Sturrock P. A., 1971, ApJ, 164, 529
Tsytovich V. N., Shvartsburg A. B., 1966, Sov. Phys. JETP, 22, 554
von Hoensbroech A., Lesch H., Kunzl T., 1998, A&A, 336, 209
Weiland J., Wilhelmsson H., 1977, Coherent Non-Linear Interaction of Waves in Plasmas. Pergamon Press, Oxford, p. 60

This paper has been typeset from a TEX/LATEX file prepared by the author.